Phase transitions at *n*-alkane/solid interfaces

M. S. Yeganeh
Corporate Strategic Research, ExxonMobil Research and Engineering Company, Annandale, New Jersey 08801
(Received 5 August 2002; published 30 October 2002)

The phase transition and molecular arrangement of various *n*-alkane/Al_2O_3 interfaces were studied using sum frequency generation spectroscopy. It was shown that a solid substrate, as opposed to air or vacuum, does not change the transition temperatures of *n*-alkanes from their bulk values. Two main phase transitions were observed. Solid *n*-alkanes, in both interface phases, lie on a substrate in a multilayer geometry with the C-C axis parallel to the interface and the molecular plane perpendicular to the substrate normal. This arrangement is different than that for monolayer systems or *n*-alkane/air interfaces.

DOI: 10.1103/PhysRevE.66.041607 PACS number(s): 68.35.−p, 42.65.Ky, 64.70.Kb

Bulk and surface phase transitions of *n*-alkanes [$CH_3(CH_2)_{n-2}CH_3$, denoted as C_n] have attracted intense research efforts for nearly a century due to their relevance to lipids, surfactants, liquid crystals, polymers, lubricants, and fuels. At temperatures above the melting point, T_m, the bulk of *n*-alkanes is in a liquid form with many conformational defects. Just below T_m many *n*-alkanes exhibit an intermediate solid phase between crystalline and isotropic liquid, known as the rotator phase [1,2]. For these materials, T_m is synonymous with the bulk liquid-rotator transition temperature T^b_{LR}. Finally, at temperatures below the bulk rotator-crystalline transition temperature T^b_{RX}, *n*-alkanes become crystalline. The C_n molecule is known to be nearly free of any conformational defects at temperatures below T^b_{LR}. The surface of some *n*-alkanes exhibits different phase behaviors than that of the bulk. For example, the surface of C_{21} shows a solid behavior with *all-trans* chains at about 3 °C above the bulk melting temperature [3–5].

In addition to the significance of the bulk and surface of *n*-alkane, the behavior of this material at solid/organic interfaces is critically important in its own right. Inhomogeneous nucleation, wetting, thin film boundary lubrication, surface deposition, and refinery fouling are just a few examples of the roles played by solid/C_n interfaces. Despite this importance, the behavior of *n*-alkane at solid/alkane interfaces has not been fully explored, and our knowledge is limited to monolayer systems and theoretical simulations [6,7].

With the development of sum frequency generation (SFG) spectroscopy, particularly IR-visible (infrared-visible) SFG spectroscopy, the inspection of solid/solid [8] and solid/liquid [9] interfaces became a possible task. IR-visible SFG is a vibrational probe sensitive to molecular compositions and interfacial structure. We have used SFG spectroscopy to examine the phase transition and molecular arrangement of *n*-alkanes at *n*-alkane/Al_2O_3 interfaces. We have observed two main interface phase transitions. The first interface phase transition is identified by a dramatic rearrangement and reconfiguration of the molecules at the interface, and it occurs at the bulk liquid-rotator transition temperature T^b_{LR}. The second interface phase transition takes place with a competition between bulk and interface nucleation at the bulk rotator-crystalline transition temperature T^b_{RX}. Only the second phase transition shows detectable hysteresis. Our polarization dependence measurements reveal that at temperatures below T^b_{LR}, in both interface phases, *n*-alkanes lie down on the substrate with their C-C axis parallel to the interface and the molecular plane perpendicular to the substrate normal in a multilayer geometry. This molecular arrangement is different than what was reported previously for monolayer systems of *n*-alkanes on various substrates [7,10]; however, the multilayer geometry is in agreement with the molecular dynamics calculation carried out on thin films of C_{16} [11].

SFG spectroscopy was carried out on C_{21}, C_{22}, C_{23}, and mixtures of C_{25}/C_{23} and C_{21}/C_{16}. An SFG cell was fabricated by clamping an equilateral Al_2O_3 (sapphire) prism against a steel backing machined with a 1-mm hollow recess to hold the *n*-alkane sample. The SFG signals were generated at the interface of the solid prism and the *n*-alkane in a total-internal-reflection geometry. The layout and details of our nanosecond SFG system have been described previously [12]. The temperature of the cell was adjusted and monitored to greater than 0.25 °C accuracy. The temperature calibration was conducted by monitoring bulk structural changes using the intensity of the reflected IR beam in an attenuated total internal geometry (ATIR spectroscopy) and differential scanning calorimetry (DSC).

Although our studies were carried out on several *n*-alkanes and their mixtures, we will focus mainly on the C_{21} results ($T^b_{LR}=39.5$ °C, $T^b_{RX}=30.5$ °C, and $T^b_{XR}=31.5$ °C) and will note the differences and similarities between C_{21} and the other systems studied where appropriate. In Fig. 1 we have plotted the SFG spectra of C_{21}/Al_2O_3 at 45 ($>T^b_{LR}$), 35 ($<T^b_{LR}$, and $>T^b_{RX}$), and 28 °C ($<T^b_{RX}$), in both *ssp* (SF is in *s*, visible is in *s*, and IR is in *p* polarization) and *sps* polarization configurations. Even a cursory inspection of the data reveals dramatic differences between spectral features, and thus the molecular structure of *n*-alkane at the organic/Al_2O_3 interface above and below T^b_{LR}. The SFG spectrum also changes in both features and intensities when the temperature of the sample drops from 35 ($>T^b_{RX}$) to 28 °C ($<T^b_{RX}$). The details of the SFG spectra of the methyl and methylene symmetric stretches of C_{21}/Al_2O_3 at 29 (labeled I) and 32 °C (labeled II) are shown in the inset of Fig. 1. Standard curve fitting results of these structures indicate that the resonance feature at 2872 cm^{-1} (the methyl symmetric stretch) sharpens, and the peak posi-

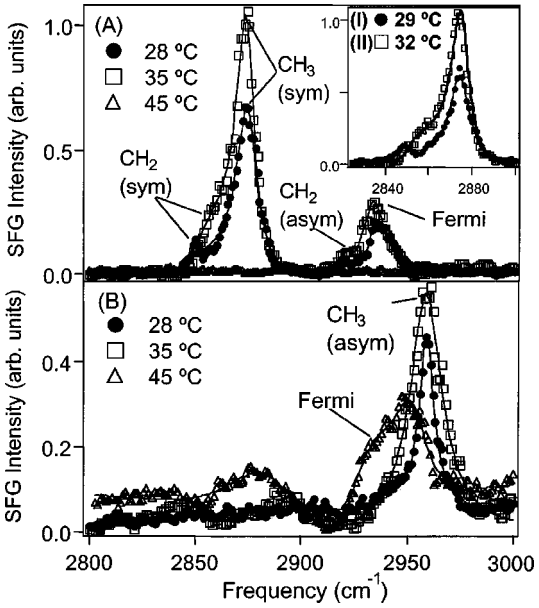

FIG. 1. SFG spectra of C_{21}/Al_2O_3 at temperatures above T^b_{LR} (△), between T^b_{LR}, and T^b_{RX} (□), and below T^b_{RX} (●) in *ssp* (A) and *sps* (B) polarization configurations. Inset: high resolution SFG spectra of methyl and methylene symmetric stretch of C_{21}/Al_2O_3 at 29 (I) and 32 °C (II). All SFG spectra recorded below 30 °C are identical to spectrum I, and all spectra recorded from 32 to 39 °C are identical to spectrum II.

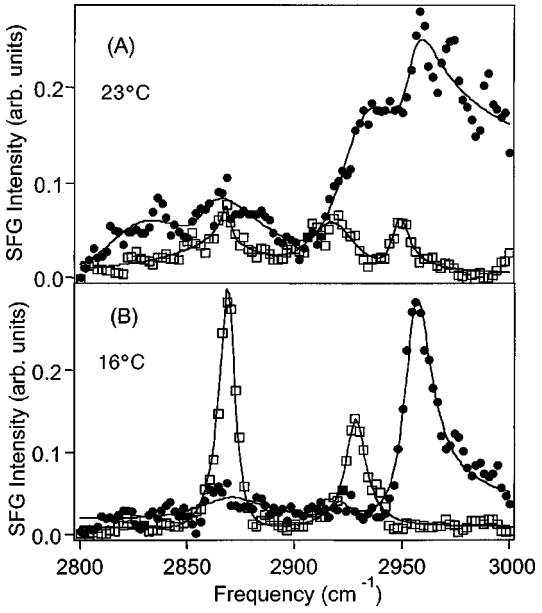

FIG. 2. SFG spectra of a C_{16}:C_{21} mixture at a mole ratio of 1/50 in *ssp*(□) and *sps* (●) polarization configurations.

tion of the methylene symmetric peak ($\sim$2850 cm^{-1}) redshifts when the temperature drops below T^b_{RX}. These findings are indications of better structural ordering and changes in the molecular environment at the alkane/solid interface.

The SFG spectra can, in principle, contain contributions from higher-order bulk nonlinearities. To investigate this effect and confirm the spatial origin of the SFG signals, we modified the Al_2O_3 surface using a coating of benzoic acid, (Tridecafluoro-1,1,2,2-tetrahydrooctyl) trichlorosilane, and water. These modifications greatly affect the SFG spectra and demonstrate that the bulk makes no contribution to the detected SFG signals. Furthermore, addition of C_{16} to C_{21} at a mole fraction of 1/50 does not change the bulk phase transition markedly, as was determined with DSC and ATIR spectroscopy. However, it does drastically alter the *n*-alkane/Al_2O_3 interface structure. Figure 2 displays the SFG spectra of the C_{16}:C_{21} mixture at 23 and 16 °C. The mixture at the organic/Al_2O_3 interface is liquidlike [Fig. 2(a)] even at 23 °C, well below the T^b_{RX} of C_{21}. It becomes solidlike only when the temperature drops below the T_m of C_{16}, as shown in Fig. 2(b). After comparing the SFG spectra with the DSC and ATIR results, one concludes that the SFG signal indeed originates at the *n*-alkane/Al_2O_3 interface.

Now that the spatial origin of the SFG signal is established, the interface transition temperatures can be determined. This was done by monitoring the SFG intensity of the methyl symmetric stretch (2872 cm^{-1}) as a function of temperature in *ssp* polarization. The heating and cooling rate was set to 0.25 °C/min and the sample was kept at the desired temperature for 10 min before data acquisition. The SFG result, shown in Fig. 3, has been normalized to the changes in the IR, visible, and SF intensities due to variation in the index of reflection of C_{21} with temperature. Sudden variations in the SFG intensities at 30.5, 31.5, and 39.5 °C represent transitions in molecular arrangement and structural changes at the interface. As seen in Fig. 3, no hysteresis was observed at 39.5 °C; however, one degree of hysteresis was detected at 30.5 °C. The values of the transition temperatures were determined from a plot of the derivative of intensity with respect to temperature, depicted in the inset in Fig. 3. It should be noted that the detected transition temperatures are the same as the bulk liquid-rotator (39.5 °C), rotator-crystalline (30.5 °C), and crystalline-rotator (31.5 °C) tran-

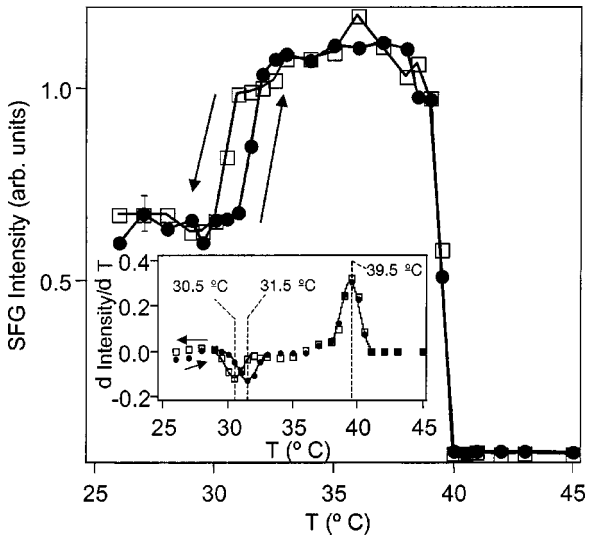

FIG. 3. The variation in SFG signal intensity with temperature of the methyl symmetric stretch of C_{21}/Al_2O_3 in *ssp* polarization. The uncertainty in SFG intensity is shown. Inset: the derivative of this variation with respect to temperature.

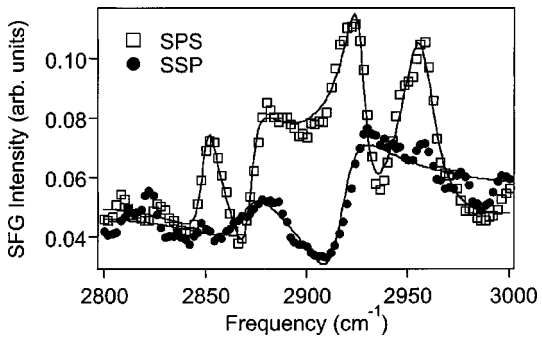

FIG. 4. SFG spectra of the C_{22}/Al_2O_3 interface. The strong resonance features are attributed to a high degree of conformational defects in *n*-alkane at the liquid/solid interface.

sition temperatures. Similar *R-X* and liquid-rotator (L-R) transition behaviors were detected for C_{23},C_{22}, and a 1:1 mixture of C_{23}/C_{25}. Therefore, the Al_2O_3 substrate does not change the transition temperatures of *n*-alkanes from their bulk values. This is different than what was observed at the free surface of *n*-alkane where the L-R transition temperature is shifted to a higher temperature by $\sim 3\,^{\circ}C$ [3–5]. The shift in transition temperature at the free surface was explained via the changes in the surface free energy [13]. A similar approach for the *n*-alkane/solid interface at, for example, $T > T_{RL}^{b}$, indicates that $\gamma_{LS} + \gamma_{SS'} - \gamma_{LS'} > 0$ (where γ is the interfacial free energy, *S* is the solid alkane, and *S'* is the solid substrate). For a relatively small value of γ_{LS} (<4 mN/m) [13], our result (i.e., no induced change in transition temperature by the substrate) suggests that the interfacial free energy of the solid alkane/substrate is greater than that of the liquid alkane/substrate for all $T > T_{RL}^{b}$. A similar argument can be made for *R-X* transition. This phenomenon may be due in part to the molecular arrangement of these materials at the solid interface. To determine the exact physical reason, a systematic study of phase transition as a function of substrate surface energy is in progress in our laboratory.

Next, we will focus on the detailed orientation and molecular arrangement of *n*-alkane in various phases, beginning with the liquid alkane/Al_2O_3 interface. It is known that the thermal energy of bulk *n*-alkane at temperatures above T_{LR}^{b} causes conformational defects in the molecular structure [14,15]. This structure is different than the linear *all-trans* configuration of the molecule at low temperatures. To identify the type of structure at the interface between C_n and Al_2O_3, it is best to use an even number *n*-alkane. This is due to the fact that an even C_n (i.e., *n* is an even number) molecule with an *all-trans* configuration is centrosymmetric, thus the SFG signals generated by the CH_2 and CH_3 groups are vanishingly small. Similarly, an even C_n with a high degree of conformational defects would exhibit strong SFG resonance features. Figure 4 shows the SFG spectrum of C_{22}/Al_2O_3 at $48\,^{\circ}C$ ($> T_{LR}^{b}$ of C_{22}). The spectra exhibit strong resonance features, which indicates that *n*-alkane at the liquid/solid interface contains a high degree of conformational defects. It should be noted that the signal intensities of C_{22} in the solid phase are an order of magnitude smaller than

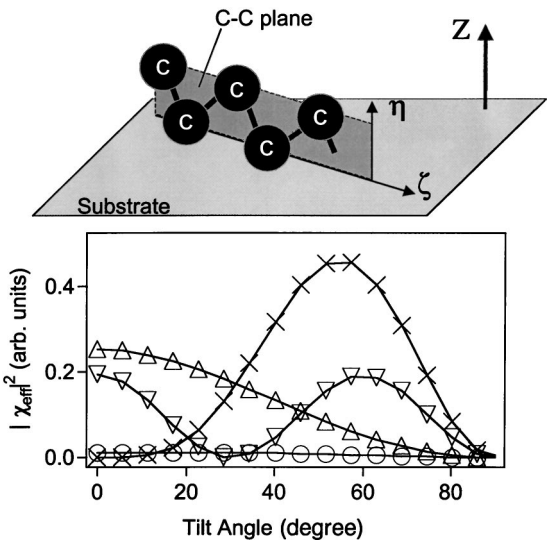

FIG. 5. The calculated variation of the square of the effective susceptibility of an odd *n*-alkane with tilt angle for symmetric *sps*(○), symmetric *ssp*(△), asymmetric *sps* (▽), and asymmetric *ssp*(×). Tilt angle is the angle between *Z* and η as the molecule rotates about ξ. ξ is the unit axis located in the molecular plane and parallel to the direction of the chain, η is a unit axis in the molecular plane perpendicular to ξ, and *Z* is the unit axis normal to the substrate. A molecule of *n*-alkane with zero tilt angle is also shown.

C_{21} and C_{23}, indicating an all-*trans* configuration of C_{22} in its solid phases. Due to this constraint on signal intensity, molecular orientation of a solid *n*-alkane must be conducted with an odd C_n.

The molecular orientation of an all-*trans* odd *n*-alkane at temperatures below T_{LR}^{b} can be determined using the SFG signal intensity of the methyl groups in *ssp* and *sps* polarizations. The signal intensity of the methyl groups depends linearly on the square of the effective second-order susceptibility of both methyl groups, $|\chi_{eff}^{(2)}|^2$, which itself contains information on the molecular orientation. We have calculated $|\chi_{eff}^{(2)}|^2$ for *ssp* and *sps* polarization for both the symmetric and asymmetric stretches of the methyl groups using an additive hyperpolarizability-based methodology. In this model, the second-order susceptibility of a single CH_3 as a function of the C-H hyperpolarizabilities was calculated in the methyl frame of reference and then transformed to an odd *n*-alkane molecular frame. The effective susceptibility was calculated by summing the susceptibility of two terminal CH_3 groups. In Fig. 5 we have plotted $|\chi_{eff}^{(2)}|^2$ of an odd *n*-alkane for both symmetric and asymmetric CH_3 with *ssp* and *sps* polarization configurations as a function of θ. In this calculation, the C-C axis (ξ in Fig. 5) is in the substrate plane, and θ is the angle between the substrate normal (*Z* in Fig. 5) and the axis that is located in the molecular plane and perpendicular to the direction of the chain (η in Fig. 5). It can be seen that with a tilt angle close to zero all experimental observations are reproduced from the calculation, that is the symmetric (asymmetric) stretch of the methyl group, detectable only in the *ssp*(*sps*) polarization configuration, and the methyl symmetric stretch that has a signal intensity greater than that of the asymmetric stretch.

We also examined a model in which the C-C axis was not in the substrate plane. In this configuration each terminal methyl group experiences a different environment; therefore, the signal of CH_3 from each end of the molecule was weighted differently. This model did not reproduce the experimental observations. In addition, we did not observe any significant changes in the ratio of the spectral features when a deuterated *n*-alkane on an OTS (octadecyl trichlorosilane) coated surface was used. Based on the above, we conclude that solid *n*-alkanes lie on the substrate with the C-C axis parallel to the interface and the molecular plane perpendicular to the substrate normal, as depicted in the inset of Fig. 5.

In order to provide a better picture of the molecular arrangements at C_n/Al_2O_3 interfaces, we have compared the methyl signal intensity of solid *n*-alkane/Al_2O_3 to OTS/Al_2O_3 and stearic acid/Al_2O_3 systems. The SFG intensity of the methyl groups of C_{21}/Al_2O_3 is comparable to those of the OTS and stearic acid/Al_2O_3. In addition, the values of the methyl effective susceptibility of C_{21}, OTS, and stearic acid are approximately identical. Since the SFG intensity depends linearly on the square of the susceptibility and the number density of the molecule, we conclude that the number of molecules generating the SFG signal in a monolayer of OTS or stearic acid must be the same as that of C_{21}. However, the number density of the vertically oriented OTS and stearic acid monolayer is far greater than that of a horizontally oriented *n*-alkane layer. This suggests that the SFG signal intensity of *n*-alkane must be generated from several layers of the organic molecule at the interface. This multilayer geometry is in agreement with the molecular dynamics calculation carried out on solid C_{16} films. It was shown that C_{16} molecules in the first four layers lie preferentially parallel to the surface [11].

We also observed that the intensity of the resonance features at 2872 cm^{-1} reduces drastically when the *R-X* transition occurs. Since the orientation of molecules remains unchanged during the *R-X* transition, we believe that the detected number of molecules is reduced during this transition. This reduction is further enhanced when an ultrasmooth substrate (rms roughness of 5 Å as determined by the atomic force microscope) was used or the temperature of the organic material was rapidly reduced from above T_{LR}^{b} to below T_{RX}^{b}. These observations indicate that the reduction in signal intensity at *R-X* is due to the competition between bulk and interface nucleation. If the interface nucleation rate is slower or the number of interfacial nucleation centers is lower than that of the bulk, then fewer layers of the molecule will orient at the interface and the SFG signal intensity will drop.

The results presented in this paper indicate that *n*-alkanes at an organic/Al_2O_3 interface undergo two main interface phase transitions which occur at T_{LR}^{b} and T_{RX}^{b}. The interfacial *n*-alkane possesses a high degree of conformational defects for temperatures above the bulk melting temperature. Solid *n*-alkane lies on a substrate in a multilayer geometry with the C-C axis parallel to the interface and the molecular plane perpendicular to the substrate normal.

We would like to thank E. B. Sirota for many stimulating discussions and M. Varma-Nair for DSC measurements.

[1] A. Muller, Proc. R. Soc. London, Ser. A **138**, 514 (1932).
[2] E. B. Sirota *et al.*, J. Chem. Phys. **101**, 10873 (1994), and references therein.
[3] X. Z. Wu *et al.*, Phys. Rev. Lett. **70**, 958 (1993).
[4] X. Z. Wu *et al.*, Science **261**, 1018 (1993).
[5] G. A. Sefler, Q. Du, P. B. Miranda, and Y. R. Shen, Chem. Phys. Lett. **235**, 347 (1995).
[6] T. K. Xia *et al.*, Phys. Rev. Lett. **69**, 1967 (1992).
[7] K. W. Herwig *et al.*, Phys. Rev. Lett. **75**, 3154 (1995).
[8] K. S. Gautam *et al.*, Phys. Rev. Lett. **85**, 3854 (2000).
[9] P. B. Miranda *et al.*, J. Phys. Chem. B **103**, 3292 (1999), and references therein.
[10] C. Merkl *et al.*, Phys. Rev. Lett. **79**, 4625 (1997).
[11] T. K. Xia *et al.*, Phys. Rev. B **48**, 11313 (1993).
[12] M. S. Yeganeh *et al.*, Thin Solid Films **270**, 226 (1995).
[13] E. B. Sirota *et al.*, Phys. Rev. Lett. **79**, 531 (1997).
[14] S. V. Naidu and F. A. Smith, J. Phys.: Condens. Matter **6**, 3865 (1994).
[15] Yesook Kim, H. L. Strauss, and R. G. Snyder, J. Phys. Chem. **93**, 7520 (1989).